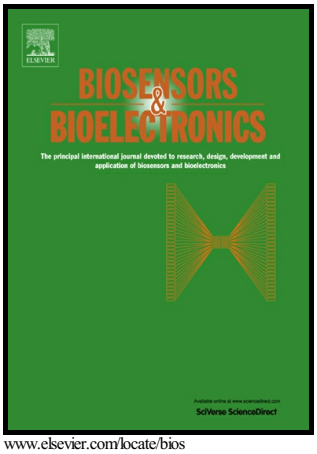

www.elsevier.com/locate/bios

Integration of biosensors into digital microfluidics: impact of hydrophilic surface of biosensors on droplet manipulation

Ehsan Samiei, George S. Luka, Homayoun Najjaran, Mina Hoorfar

PII: S0956-5663(16)30226-3
DOI: http://dx.doi.org/10.1016/j.bios.2016.03.035
Reference: BIOS8546

To appear in: *Biosensors and Bioelectronic*

Received date: 14 January 2016
Revised date: 14 March 2016
Accepted date: 16 March 2016

Cite this article as: Ehsan Samiei, George S. Luka, Homayoun Najjaran and Mina Hoorfar, Integration of biosensors into digital microfluidics: impact of hydrophilic surface of biosensors on droplet manipulation, *Biosensors and Bioelectronic,* http://dx.doi.org/10.1016/j.bios.2016.03.035

Integration of biosensors into digital microfluidics: impact of hydrophilic surface of biosensors on droplet manipulation

Ehsan Samiei, George S. Luka, Homayoun Najjaran, and Mina Hoorfar*

University of British Columbia, 3333 University way, Kelowna, BC V1V1V6, Canada

Email address: mina.hoorfar@ubc.ca

*Corresponding author: Mina Hoorfar

Abstract

Several studies have been performed on the integration of biosensors into digital microfluidics (DMF). Despite the general success in their detection capabilities, there are still two challenges associated with the integration of biosensors into DMF: 1) complete removal of the droplet containing the analytes from the sensing surface; and 2) biochemical regeneration of the biosensor involving detaching the target analyte from the receptor after each round of sensing. The latter is case dependent and the solution can vary from one application to another. Our research aims at addressing the former, the solution to which is applicable to all biosensors integrated to DMF. This paper presents a thorough characterization of the hydrophilic surface of the biosensor in terms of wettability and geometry, taking into account the overall configuration of the DMF platform. Consequently, we identify the optimal geometry of the sensing surface and the DMF platform providing successful removal of the target droplet from the sensing surface after detection. Based on the results, the gap height is suggested to be chosen at the upper limit of the applicable range. Also, the biosensor, patterned on the device top plate, is recommended to be designed with a high aspect ratio and aligned with the center of the actuating electrode. As a proof of concept, the optimum configuration is implemented on a DMF platform with an interdigitated capacitive biosensor to detect different concentrations of *Cryptosporidium*, for which it is shown that the sample droplet is removed successfully from the superhydrophilic surface of the biosensor.

Keywords: Digital microfluidics; Biosensor; Hydrophilic surface; Capacitive detection.

1- Introduction

Manipulation of small droplets of liquids has been used as a powerful mean to perform biochemical experiments on so-called digital microfluidic (DMF) devices (Choi et al, 2012; Fair, 2007). In such systems, which are developed in either open or closed (sandwiched) configurations (Yi and Kim, 2006; Fan et al., 2009), the manipulation of samples is performed in the form of droplets on an array of electrodes which are addressable individually. Sample manipulation is performed on DMF platforms by the aid of four basic operations including droplet transport, mixing, splitting and dispensing (Cho et al., 2003; Samiei and Hoorfar, 2015). Multiple actuation methods have been used for droplet manipulation on such systems (Mugele and Baret, 2005); yet electrowetting on dielectric (EWOD) is the most common method due to its reliability and robustness (Fair, 2007; Mugele and Baret, 2005).

DMF has been widely used in biochemical applications due to the recent advances made in applying antifouling techniques to these devices (Luk et al., 2008). In general, biochemical applications, found in numerous studies (Choi et al, 2012; Samiei et al., 2015; Fair et al., 2007; Rakus et al., 2015; Rezaei Nejad et al., 2015), require detection of one or multiple targets in a medium. While in off-line detection mode (Malic et al., 2010), the detection has been performed off the chip, in the on-line mode, which is of particular interest for performing the entire assay on the chip (Choi et al., 2012; Luka et al., 2015) especially for point-of-care applications, the detection is performed on the chip. For on-line detection methods, the sensing surface of the sensor (functionalized with biological receptors) is in direct contact with the sample. This requires the removal of certain parts of the hydrophobic layer on the DMF device (Malic et al., 2011; Choi et al., 2012). This consequently limits droplet manipulation. On-chip detection of multiple different analytes has been successfully shown in several studies (Malic et al., 2010). However, two main challenges associated with the integration of biosensors into DMF are yet to be addressed: 1) sample removal from the hydrophilic surface of the biosensor; and 2) biochemical regeneration of the biosensor (detaching the target analyte from the receptor) after each round of sensing. While the latter is case dependent and the solution can vary from one application to another, the solution found for the former problem can be applied to all types of biosensors. In multiple studies in which such detection methods have been adopted, the sensing surface has been kept small enough to enhance droplet transport over the sensing surface (Malic et al., 2011; Choi et al., 2012; Yu et al., 2014). For instance, Yu et al. (2014) limited the area of the sensing surface to 9.6% of the area of the actuating electrodes for successful droplet removal from the sensing zone. However, the performance of the sensor might be hindered by limiting its surface area. Therefore, a systematic study is needed to find the optimum geometry for such detection systems on DMF to use the largest possible area for sensing surface.

In this paper, a thorough study is performed to characterize the hydrophilic surfaces of the biosensors, resulting in finding the optimum configuration of the sensing surface for successful droplet manipulation. The hydrophilic spots (HS) which represent the sensing surface of the biosensors are patterned in a rectangular configuration on the top plate (a possible location for patterning the sensor) and positioned on the top of the array of electrodes on the bottom plate. Three common surface materials in biosensors are selected for HS: gold (Au), silicon dioxide (SiO_2) and Au with immobilized antibodies (Au_m). The main goal is to find the best configuration of HS and the DMF system (resulting in largest size of the sensor) for which droplet transport is performed with the notion of negligible sample residual on HS. As a proof of concept, the optimized geometry found for the HS and the best configuration for the DMF device are used to fabricate a capacitive-based biosensor (Berggren et al., 2001; Alizadeh et al., 2013) for detection of *Cryptosporidium*. Two main criteria used for evaluating the success of the biosensor developed are the removal of the sample from the sensing area after detection and the capability of the sensor to detect the target.

2- Experimental procedure

In this paper, the detection system is integrated on the top plate of the DMF device and positioned on top of the array of electrodes patterned on the bottom plate. A rectangular shape is chosen for the hydrophilic spot (HS), representing the sensing surface of the sensor. The schematic of the device is illustrated in Fig. 1a. To perform a thorough characterization of HS, the experiments have been performed in three stages. First, the surface properties of different surfaces chosen for HS (i.e., Au, SiO_2 and Au_m) are studied by contact angle measurement. In the next step, droplet transport on a DMF device is performed over HS areas with different geometrical and surface properties to find the best geometry over which a droplet can be transported with no or a negligible residual volume on HS. Finally, based on the optimum configuration found for HS, a capacitive biosensor is fabricated for the detection of a target (*Cryptosporidium* in this case) on a DMF device such that after the detection process the droplet can be transported away from the biosensor.

Droplet actuation was performed using EWOD. A frequency of $f = 1kHz$ was used for the applied potential. The voltage was generated using a signal generator (Tektronix AFG3021B0) in series with an amplifier (TREK PZD700). The experiments were monitored under a microscope (Leica Z6 APO) and recorded using a high speed camera (2592 × 1944 resolution). For all experiments, the threshold voltage (U_{th}) required for removing the droplet from the hydrophilic spot (HS) was applied. In fact, U_{th} is used to compare the results obtained for different sets of experiments. The duration of the applied voltage varies between $1 - 3s$ for different cases.

2-1- Surface properties

The hydrophilicity of the surfaces is determined by contact angle measurement (Tavana et al., 2007). The advancing (θ_{adv}), the receding (θ_{rec}), the change in the receding ($\Delta\theta_{rec}$), and the difference between the advancing and receding (θ_{hys}, contact angle hysteresis) contact angles are used for the comparison of the surface properties of different materials. An experimental setup shown in Fig. 1b is used for the contact angle measurement. Using a syringe pump (KDS LEGATO 270, KD Scientific) water is injected on to the surface through the needle (with hydrophobic surface) in multiple steps. For each step, a volume of 100 μL is injected. After each injection the contact angle is measured from the side-view image. The process continues until the contact angle does not change anymore; at that stage the measured contact angle is presented as θ_{adv}. Afterwards, the liquid on the surface is pushed back into the needle using the same approach. The contact angle continues to decrease while the three-phase contact line pins on the surface. At the verge of the motion of the three-phase contact line the contact angle measured is defined as the initial receding contact angle (θ^*_{rec}). The receding contact angle continues to decrease by further removal of the liquid until its value reaches a plateau, which is defined as the final receding contact angle (θ_{rec}). The change in the receding contact angle is calculated as $\Delta\theta_{rec} = \theta^*_{rec} - \theta_{rec}$. The contact angle hysteresis is also calculated by subtracting the receding from the advancing contact angle, $\theta_{hys} = \theta_{adv} - \theta_{rec}$.

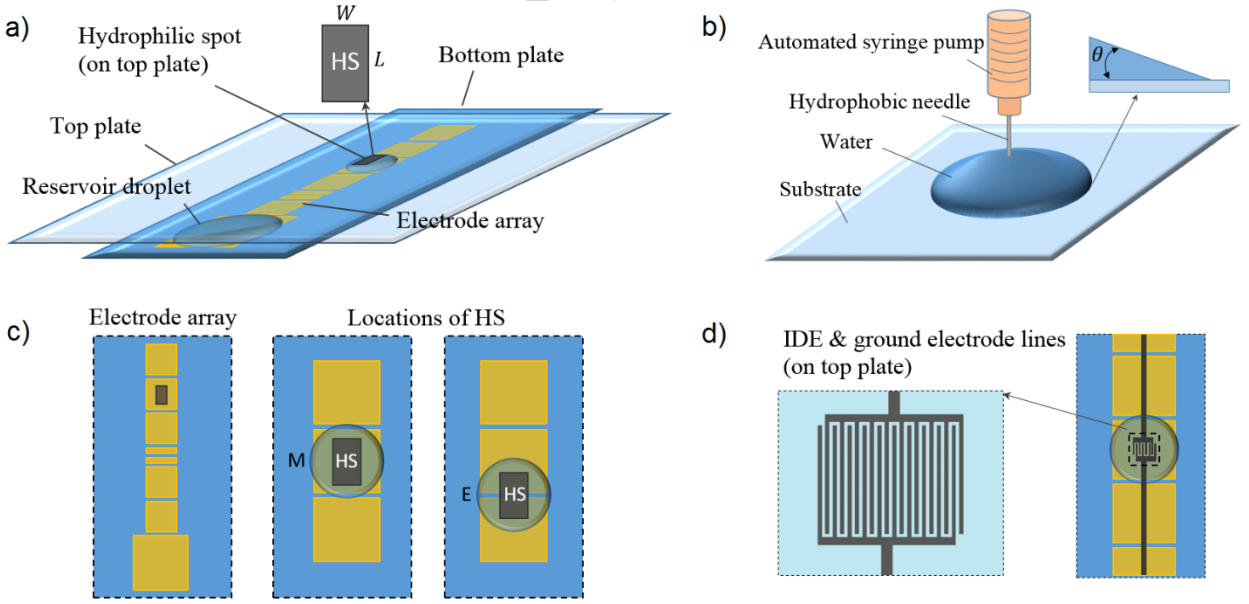

Fig. 1 a) Schematic of the DMF setup for droplet transport over a hydrophilic spot (HS), patterned on the top plate and located on the array of electrodes. b) Schematic of the experimental setup for contact angle measurement. c) Configuration of the array of electrodes for droplet manipulation and the two considered

locations for the HS (aligned with the middle (M) and the edge (E) of the bottom electrode). d) Schematic of the interdigitated electrodes (IDE) and the ground electrode located over the array of electrodes. The configuration of IDE is shown in the inset of the image.

2-2- Experiments on hydrophilic spot (HS)

The hydrophilic spot (HS) is patterned in a rectangular shape with different aspect ratios ($\gamma = 0.4, 0.667, 1, 1.5$ and 2.5) where the aspect ratio is defined as $\gamma = L/W$ (length/width of HS, Fig. 1a). A dimensionless surface area (A^*_{HS}) for HS is defined as the ratio of the area of HS (A_{HS}) to that of the actuating electrodes (A_d). Several values of A^*_{HS} are considered as $A^*_{HS} = 0.089, 0.133, 0.178$ and 0.222 which represent 8.9%, 13.3%, 17.8% and 22.2% of the area of the actuating electrodes, respectively. For the DMF system, square electrodes with two different dimensions of $L_d = 1.5$ and $2mm$ and the gap heights (between top and bottom plates) of $h = 150,\ 220$ and $280\mu m$ were chosen, while the normalized gap height is defined as $h^* = h/L_d$. Also, the sensitivity of the results to the volume of the droplet is studied with three different volumes of the droplet. To generate variable, but accurate, volumes of droplets, two of the electrodes are patterned with a smaller width ($0.185\ mm$) (Fig. 1c) and droplet dispensing from the reservoir electrode is performed by actuating different combinations of a normal electrode and the two thinner electrodes, as suggested by Samiei and Hoorfar (2015). Two possible locations are studied for HS: 1) the HS on the top plate is aligned on the middle part of the bottom electrode (referred to as M in Fig. 1c), and 2) the HS is aligned with the edge of the bottom electrode (referred to as E).

2-3- Detection

As the last stage, the droplet transport is performed over a biosensor integrated into the DMF platform for the detection of *Cryptosporidium.* This part is conducted to show the use of the optimum configuration for the sensing surface found in this study. A capacitive biosensor is patterned on the top plate (Fig. 1d), which is formed of two interdigitated electrodes (IDE) made of gold (Fig. 1d) with the immobilized antibodies specific to *Cryptosporidium*. A window of the Cytonix layer is removed from the IDE surface to expose the biosensor to the target. The capacitive measurement is performed using a network analyzer (N5241A, Agilent Technologies) in the frequency range of 4 GHz to 7 GHz. After detection, the droplet is moved away from the sensing zone to show the feasibility of the study presented here.

3- Device fabrication

The bottom plate contains the actuating electrodes for droplet manipulation, and the top plate contains the ground electrode. The detection system is patterned on the top plate and placed over the array of actuating electrodes. The hydrophilic spot (HS) under study is patterned on the top plate by partially removing the hydrophobic layer and depositing the desired material. The fabrication of the bottom and the top plates, and the biosensor used for the detection of *Cryptosporidium* are extensively explained in the Device Fabrication Section in the Supplementary Material.

4- Results and discussion

The objective of the present study is to experimentally characterize the hydrophilic surface of the sensors on DMF platforms such that droplet manipulation is performed over the sensing surface with no or a negligible amount of liquid residing on the surface. Initially, the surface properties of the sensors (HS) will be studied with three surfaces: Au, SiO_2, and Au_m. Then the geometry of HS will be studied for different configurations of the DMF platform. Finally, based on the optimum geometry, an interdigitated electrode (IDE) capacitive biosensor is integrated to the DMF platform for detection of a sample target (*Cryptosporidium*) as a proof of concept.

4-1- Surface characterization of hydrophilic spot (HS)

The ability to remove the droplets from the surface of the biosensors on DMF systems depends on the surface properties (wettability) of the biosensing region. Most sensors (e.g., electrochemical and optical) integrated into DMF devices are patterned on either glass substrates or a silicon wafer with an oxide layer grown on the surface, and formed using gold electrodes. Other plastic-based surfaces are also frequently used, though such materials are significantly less hydrophilic, and hence, less limiting than glass and SiO_2 for droplet manipulation. Therefore, Au and SiO_2 are the most appropriate choices for the hydrophilic spot (HS) in this study. However, the biological sensors are always functionalized using the bio-receptors (e.g., antibodies), specific to a certain type of target analyte. To consider this, a gold surface with immobilized antibodies (Au_m) is also characterized. Using the experimental setup shown in Fig. 1b and the procedure explained in Section 2.1, the advancing, receding, the change in the receding and the difference between the advancing and receding contact angles (θ_{adv}, θ_{rec}, $\Delta\theta_{rec}$ and θ_{hys}, respectively) are measured for the three surfaces under study. The results are presented in Table I.

Table I. Results of the contact angle measurement for the three surfaces of Au (gold), SiO2 (silicon dioxide) and Au_m (gold with immobilized antibodies).

Surface	Au	Au_m	SiO_2
$\theta_{adv}(°)$	90	56.48	21.98
$\theta_{rec}(°)$	45.94	3.82	4.22
$\Delta\theta_{rec}(°)$	1.04	10.57	4.64
$\theta_{hys}(°)$	44.06	52.66	17.76

The advancing contact angle for Au, SiO_2 and Au_m are $\theta_{adv} = 90°,\ 21.8°$ and $56.48°$, respectively. This suggests that the SiO_2 surface has a high degree of hydrophilicity. The comparison between θ_{adv} for Au and Au_m shows that the presence of the antibodies significantly decreases the advancing contact angle which is the result of the change in the surface morphology and hydrophilicity caused by the immobilization of antibodies. On the other hand, the comparison between the receding contact angles shows that Au_m and SiO_2 surfaces are superhydrophilic due to their very low receding contact angles ($\theta_{rec} = 3.82°$ and $4.22°$ for Au_m and SiO_2, respectively) while Au surface is relatively hydrophilic. The change in the receding contact angle and the contact angle hysteresis for SiO_2 surface ($\Delta\theta_{rec} = 4.64°$ and $\theta_{hys} = 17.76°$) show that the sputtered SiO_2 has a relatively smooth surface, while the other two surfaces have a rough morphology. Especially, Au_m surface has a large hysteresis ($\theta_{hys} = 52.66°$) which is due to the superhydrophilicity of the antibodies and the rough morphology of the surface. These results suggest that Au_m and SiO_2 surfaces can be considered as the most extreme cases due to their superhydrophilicity (extremely low θ_{rec}).

4-2- Geometrical optimization of hydrophilic spot (HS)

The geometry of the hydrophilic spot (HS) representing the biosensing area, was studied for different geometrical parameters. The parameters studied here are the aspect ratio (for the rectangular shape considered here), the surface area and material for HS, and the electrode size and the gap height for the DMF platform.

Effect of the size and aspect ratio of HS

In the first part, the aspect ratio (γ) and the normalized area (A^*_{HS}) of HS are studied. For this purpose, the electrode size of $L_d = 2mm$ and the gap height of $h = 220\mu m$ ($h^* = 0.11$) were considered for the DMF platform. Also, a conventional electrode (one electrode after the reservoir shown in Fig. 1c) was used to dispense the droplet of a volume of $V_d = 0.88\mu L$ for all experiments. The results illustrated in Fig. 2a show the threshold voltage (U_{th}) versus the aspect ratio of HS (γ). The first conclusion drawn from the results is that U_{th} increases as the size of HS increases. Since hydrophilicity of the surface is a limiting

factor for droplet motion, a large applied voltage is hence required for transport of a droplet over a larger HS area. For the case of the Au surface, we found that even for the largest HS area ($A^*_{HS} = 0.222$) tested here the droplet can be removed from the surface without reaching the maximum possible voltage.

The effect of the HS aspect ratio (γ) can be observed in Fig. 2a. For a certain size of HS, U_{th} is descending with respect to γ. This behavior is observed for all four HS sizes ($A^*_{HS} = 0.089, 0.133, 0.178$ and 0.222). The effect of the aspect ratio on droplet removal can also be observed from the experimental images shown in Fig. 3a. In essence, the EWOD force from the bottom-plate electrode is driving (pulling) the droplet; while HS on the top plate causes resistance in the motion of the droplet (especially around the three-phase contact line). The smaller the width of the HS (i.e., the larger γ) the smaller the resistance and consequently the smaller the value of U_{th} (as observed in Fig. 2a). Therefore, the width of HS has a dominant effect on the required voltage.

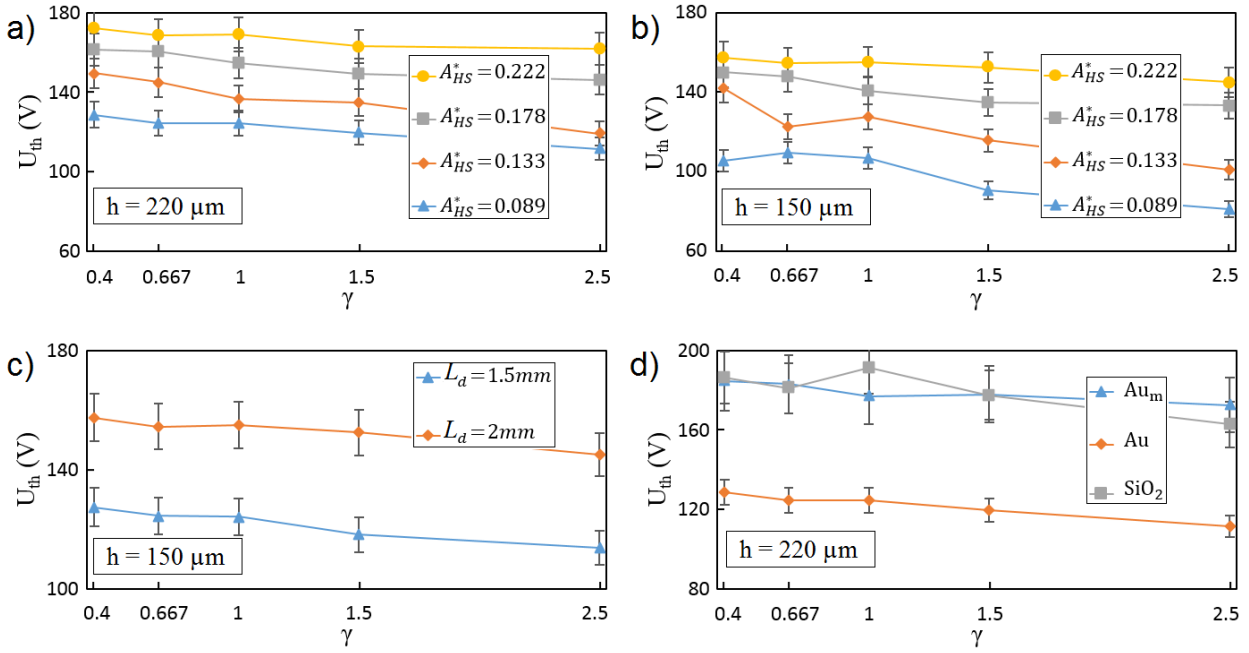

Fig. 2 Results of the experiments conducted for geometrical optimization of the hydrophilic spot (HS). All the results were obtained for a platform containing a $2mm$-electrode array and a) the gap height of $h = 220\mu m$ ($h^* = 0.11$) and the Au HS normalized areas of $A^*_{HS} = 0.089, 0.133, 0.178$ and 0.222, and b) the gap height of $h = 150\mu m$ ($h^* = 0.075$) and the Au HS normalized areas $A^*_{HS} = 0.089, 0.133, 0.178$ and 0.222. c) The graph shows the comparison between the $1.5mm$ and $2mm$ electrodes with the Au surface, $h = 150\mu m$ and $A^*_{HS} = 0.222$. d) The graph shows the comparison of the three surfaces (Au, Au_m and SiO_2) with $h = 220\mu m$ ($h^* = 0.11$) and $A^*_{HS} = 0.089$.

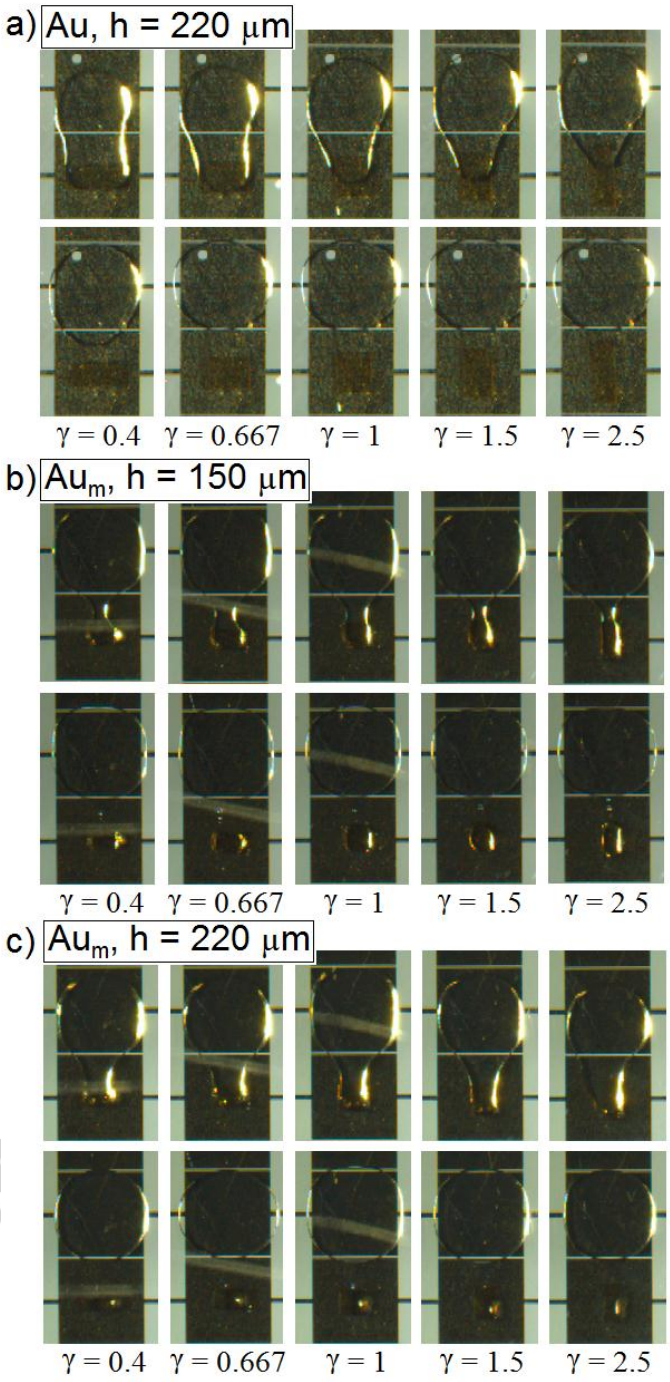

Fig. 3 Experimental images of the HS areas tested with the electrode size of $L_d = 2mm$. In each case, the top row images show the moments that the droplet is on the HS and the adjacent electrode is activated to pull away the droplet, and the bottom row images show the moment right after the droplet is pulled away for a) the gap height of $h = 220\mu m$ ($h^* = 0.11$) and the Au HS size of $A_{HS}^* = 0.222$ Au surface, b) the gap height of $h = 150\mu m$ ($h^* = 0.075$) and the Au_m HS size of $A_{HS}^* = 0.089$, and c) the gap height of $h = 220\mu m$ ($h^* = 0.11$) and the Au_m HS size of $A_{HS}^* = 0.089$.

Effect of the gap height

To study the effect of the gap height, all the experiments were repeated for the gap height of $h = 150\mu m$ ($h^* = 0.075$) and the results are shown in Fig. 2b. Using a similar method of droplet dispensing, the surface area (observed in the top view) of the droplet was kept similar to that obtained for the case of the gap height of $h = 220\mu m$ ($h^* = 0.11$). The overall trend of the curves is similar to that observed for the case of $h^* = 0.11$ (U_{th} is descending with respect to γ) except for the fact that the required applied voltage is smaller ($10 - 20\%$ smaller than U_{th} for $h^* = 0.11$). However, it has to be mentioned that decreasing the gap height does not necessarily enhance droplet removal from HS since interfacial stability of the droplet deteriorates as the gap height is decreased (Samiei and Hoorfar, 2015). This will be discussed in detail later (see the section about "Effect of the surface properties of HS").

Effect of the electrode size

The effect of the electrode size on the droplet removal has also been taken into account by comparing the results for two electrode sizes of $L_d = 1.5mm$ and $L_d = 2mm$. For this comparison the gap height is set to $h = 150\mu m$ and only the largest HS size is considered ($A^*_{HS} = 0.222$). As it could be observed in Fig. 2c, the case with the smaller electrode requires smaller U_{th} ($\sim 20\%$ lower voltage) for droplet removal from HS. This suggests that a smaller size of the electrode array has a better performance for droplet removal. However, it has to be noted that A^*_{HS} is the ratio of the HS surface area to that of the actuating electrode, and hence for a similar A^*_{HS} (for both electrode sizes), the HS size is smaller for the smaller electrode length (i.e., $L_d = 1.5mm$). This may not be desirable as the size of the biosensor is in fact independent of the DMF platform. In other words, fabrication of a certain type of sensor with a desired sensitivity requires a specific surface area which is independent of the size of the DMF actuating electrodes. Therefore, using a smaller electrode array might limit the area available for sensor fabrication.

Effect of the surface properties of HS

The electrode size of $L_d = 2mm$ was chosen for this part since it provided a larger area of HS. Initially, two gap heights of $h = 150\mu m$ and $220\mu m$ ($h^* = 0.075$ and 0.11, respectively) were used for the study. Figures 3b and 3c show the droplet images for the experiments performed with the Au_m surface with the HS size of $A^*_{HS} = 0.089$ for the two gap heights. As it can be observed in Fig. 3b representing the results for $h^* = 0.075$,, the droplet splits on the HS surface (for all cases of γ) upon pulling motion. This is due to the fact that for the lower gap heights the droplet is less stable, and since the Au_m HS is superhydrophilic the droplet will split. By increasing the gap height to $h^* = 0.11$, on the other hand, the droplet can be pulled away from the HS surface without splitting (see Fig. 3c). However, a very small

volume of liquid (in the range of $< 500pL$) remains on the HS surface (only on the top plate) with a volume less than 0.1% of the original droplet volume. This small size of the liquid can readily be removed by transporting one or two washing droplets over HS. Therefore, for successful removal of the sample droplets from the hydrophilic sensing surfaces on DMF, the gap height should be kept large enough to prevent droplet splitting. However, it has to be considered that for very large gap heights droplet dispensing from the reservoir will be hindered or produce large deviations in the droplet volumes (Samiei and Hoorfar, 2015) , affecting the reliability of bioassays performed on the chip. Therefore, the choice of the gap height is very crucial to satisfy these two problems.

Based on the above discussion, the gap height was set to $h^* = 0.11$ for the experiments with HS of Au_m and SiO_2 (superhydrophilic). Droplet removal was successful only for $A^*_{HS} = 0.089$ and it failed for $A^*_{HS} = 0.133, 0.178$ and 0.222. The results for the successful case of $A^*_{HS} = 0.089$ and $h^* = 0.11$ are shown in Fig. 2d for the three surfaces of Au, SiO_2 and Au_m. It can be observed that the threshold voltage is relatively low for the Au surface ($111 - 129V_{rms}$ for all values of γ) while it is $40 - 60\%$ larger for Au_m and SiO_2. In addition, it can be observed that for the two superhydrophilic cases (Au_m and SiO_2), the threshold voltage (U_{th}) is very similar. This is due to the fact that the receding contact angles for these two surfaces are very close ($\theta_{rec} = 3.82°$ and 4.22° for Au_m and SiO_2 surfaces, respectively). To achieve successful droplet removal from a larger HS the gap height was increased to $h = 280\mu m$ ($h^* = 0.14$) and the experiments were performed for both Au_m and SiO_2 surfaces successfully with the HS sizes of $A^*_{HS} = 0.089$ and 0.133. This shows that it is possible to transport a droplet over an HS area as big as 13.3% of the size of the actuating electrodes, while the gap height is within an acceptable range for droplet splitting on the actuating electrode of $L_d = 2mm$. For a DMF system with the electrode size of $L_d = 2mm$, this will result in an HS area of $0.73mm \times 0.73mm$, which is large enough for the fabrication of most types of biosensors including interdigitated electrode (IDE) capacitive, surface plasmon resonance (SPR), and amperometric biosensors.

Effect of the droplet volume

To study the sensitivity of the results to the volume of the droplet, a set of experiments was performed with three different volumes of the droplet. For these experiments, the electrode length of $L_d = 2mm$, the gap height of $h^* = 0.075$, and the HS surface made of Au with the aspect ratio of $\gamma = 1$ (square HS) and the normalized HS surface area of $A^*_{HS} = 0.222$ were used. Three different combinations of the electrodes were used to generate droplets with different volumes using the configuration shown in Fig. 1c.: 1) a square-shaped electrode ($V_1 = 0.71\mu L$), 2) a combination of a square-shaped electrode and a thin electrode ($V_2 = 0.85\mu L$), and 3) a square-shaped electrode and two thin electrodes ($V_3 = 0.98\mu L$). The

droplets generated using this method are shown in Fig. 4a. The droplets were transported to HS and then removed from it using threshold voltages of $U_{th} = 154.8, 155.26$ and $155.9V$, respectively. The differences between these three voltages are less than 1% which can be assumed negligible for the droplet volume changes of almost 40%.

Effect of the HS position with respect to the bottom-plate electrodes

The effect of the location of the hydrophilic spot (HS) with respect to the bottom-plate electrode was also studied. For this purpose two locations of the HS were considered as M (middle) and E (edge). Droplet removal was performed using these two locations and the experimental images are shown in Fig. 4b. The threshold voltage required to remove the droplet was $U_{th} = 150.18$ and $134.76V$ for the M and E locations, respectively. The smaller voltage for the E location suggests that this location is easier for droplet removal compared to the M location. However, due to a much longer neck formed in the case of the E location (see the left image in Fig. 4b), there is a high possibility of droplet splitting over HS. For the Au surface used for these experiments droplet splitting happened for 20% of the attempts, while for the M location all the attempts were successful and the droplet was completely removed from HS. The splitting issue for the E location will even be more probable for surfaces with higher levels of hydrophilicity (such as Au_m and SiO_2). Therefore, the M location is more reliable for placing HS.

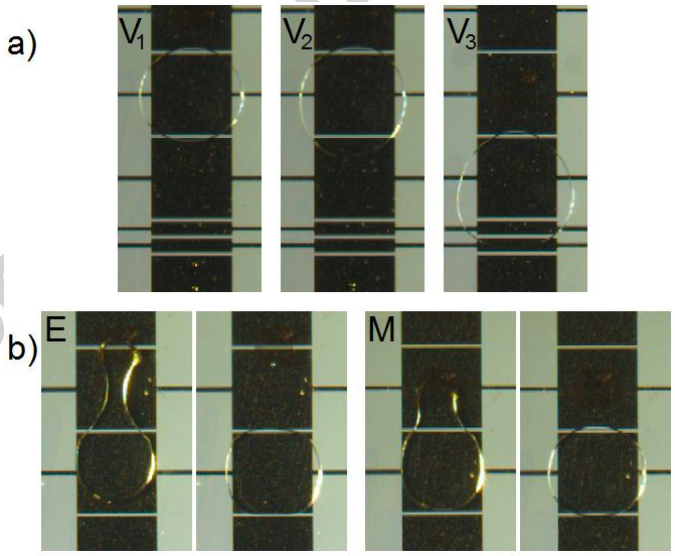

Fig. 4 a) Droplets with three different volumes generated using 1) a square-shaped electrode ($V_1 = 0.71\mu L$), 2) a combination of a square-shaped electrode and a thin electrode ($V_2 = 0.85\mu L$), and 3) a combination of a square-shaped electrode and two thin electrodes ($V_3 = 0.98\mu L$). b) The experimental images for two locations of the HS: 1) the HS was aligned with the middle of the actuating electrode on

the bottom plate (referred to as the M location), and 2) the HS was aligned with the edge of the actuating electrode on the bottom plate (referred to as the E location). In each of these images (labeled as E and M), the left image shows the droplet before removal and the right image shows the droplet after removal from the HS area.

4-3- Capacitive biosensor for detection of *Cryptosporidium*

Manipulation of a droplet over a hydrophilic spot (HS) was studied thoroughly in the previous part of this paper and the effects of multiple parameters including the type and the geometry of HS and the DMF system on the limits of droplet transport were discussed. Considering the optimum dimensions found for HS and the corresponding configuration for the DMF system, a biosensor is fabricated and integrated into DMF to examine the feasibility of performing on-chip sample sensing and removal of the sample from the sensing surface afterwards. For the proof of concept, detection of *Cryptosporidium* is performed with an interdigitated electrode (IDE) capacitive biosensor with the geometry explained in Section 2 (Fig. 5a). Detection of *Cryptosporidium* is chosen for this test because the protein compounds used for the linker along with the immobilized antibodies and incubated cells provide the highest level of hydrophilicity which can be considered as an extreme case for droplet removal. The gap height for the DMF device is set to $h = 280\mu m$ ($h^* = 0.14$) and the electrode array with the size of $L_d = 2mm$ is used for the experiment. As explained earlier, the top plate is a glass slide containing the IDE sensor. The top plate is covered with a hydrophobic layer facilitating droplet manipulation. To expose the sensing part (the IDE area), a square window with the size of $0.73mm \times 0.73mm$ (The largest size compatible with $h^* = 0.14$ and the Au_m surface) was removed from the hydrophobic layer. The connection lines of IDE are used as the ground electrode for droplet transport to the sensing zone (IDE). After transporting the droplet to the sensing zone, the connection lines are detached from the signal generator (used for droplet manipulation) and then connected to the network analyzer for sensing.

Capacitive sensing was conducted for a sample of DI water on the IDE in the DMF setup shown in Fig. 5a. Measurements were performed first for the IDE with immobilized anti-*Cryptosporidium* antibodies (C_0) and then with the IDE incubated with *Cryptosporidium* (C). For each case the capacitance was measured after delivering a droplet of water to the IDE area. Fig. 5b shows the difference between the capacitance of the IDE with and without the cells, normalized with the capacitance without the cells ($\Delta C/C_0 \times 100$ (%)), for five different concentrations of *Cryptosporidium* in a range between 15 cell/μL to 240 cell/μL (C15 to C240). The measurements were carried out for eight replications of each concentration and the average values and the standard deviations from the average were calculated. The

results in Fig. 5b show that for the chosen range of frequency the difference in capacitance increases as the frequency is increased. Also, the measured signal increases as the concentration of the sample increases. The calibration curve is provided in Fig. 5c. Based on this graph, the increase in the signal by increasing the number of cells is faster for lower concentrations, while the slope of the curve becomes smaller for higher concentrations.

For all measurements, the water droplet was transported to the sensing zone (IDE) and after the measurement the droplet was successfully transported away from IDE (Fig. 5a). This illustrates feasibility of droplet removal from the hydrophilic biosensing surfaces in DMF systems.

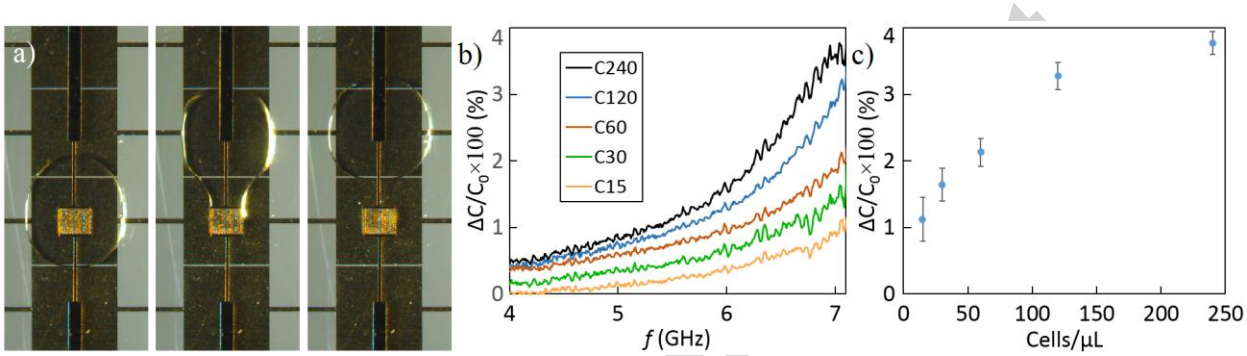

Fig. 5 Results of the capacitance measurement for detection of *Cryptosporidium*. The measurements are performed with water as the medium and the frequency range of $f = 4GHs$ to $7GHz$. a) A Sequence of images showing detection and droplet removal from the IDE biosensor located on the top plate is illustrated. b) Capacitive measurements for the samples with different concentrations of cells, ranging from 15 cell/μL to 240 cell/μL. ΔC presents the difference between the measured capacitance of the IDE incubated with the solutions of cells (C) and the IDE with immobilized antibodies (C_0). c) The calibration curve for the results is presented for 8 replications conducted for each concentration. The error bars present the standard deviation of the results from the average value.

4-4- Discussion

The transport of droplets over hydrophilic spots (HS) was performed for different surface properties and geometry of the HS and DMF platform. It was shown that certain strategies have to be considered for designing the geometry of the sensing surface of the biosensors and setting the parameters of the DMF platform to achieve the largest possible size of the surface for successful droplet removal after biosensing. Based on the results shown in this paper, it is recommended to design the sensing surface with a high aspect ratio and align it with the center of the actuating electrode. In fact, the distance between the edge of the sensing surface and the edge of the following actuating electrode should be kept less than half of the

length of the electrode to avoid excessive elongation and breakup of the droplet. The gap height for the DMF system is dependent to the fabrication of the device. To avoid droplet breakup, it is recommended to keep the gap close to the upper limit of the range required for precise droplet manipulation.

5- Conclusions

To apply the digital microfluidic (DMF) systems to practical biochemical aplications and utilize them in assays requiring the detection of target analytes, one main concern is the ability to restore the sensing surface. This requires that the sample droplet be removed and the sensing surface on the chip be completely cleared with negligible or preferably no residual volume left behind. In practice, this concern has limited the use of DMF systems as a complete micro-total analysis system since liquid manipulation requires hydrophobic surfaces whereas the sensing surfaces of biochemical sensors typically demand hydrophilic surfaces. In the present work, a systematic study was conducted to find the optimal geometry for a hydrophilic spot (HS), representing the sensing surface of a sensor, and the overall configuration of the DMF platform using which it is possible to remove the droplets from HS. A rectangular geometry is considered for HS with the aspect ratio (γ =length / width) ranging between $0.4 < \gamma < 2.5$. Three different surface materials of gold (Au), silicon dioxide (SiO_2) and gold with immobilized antibodies (Au_m) were tested. The effects of the electrode size and the gap height between the two plates of the DMF system were also studied. The dominant parameters were found to be the aspect ratio of HS, the gap height in the DMF platform, and the location of HS with respect to the actuating electrodes in DMF. Results revealed that the higher the aspect ratio of the HS the lower the threshold voltage (U_{th}). It was also found that a decrease in the width of HS reduces U_{th}. The study of the gap height between the two plates (h) showed that reducing h decrease U_{th}. However, lowering h also decreases the stability of the droplet, increasing the chance of splitting over HS. Therefore, h has to be kept within a certain range (depending on the device properties, here $h^* = h/L_d = 0.14$ where L_d is the electrode size) to enhance droplet removal, and also perform droplet generation with an acceptable precision. Also, two different locations tested for HS showed that aligning HS with the middle part of the actuating electrode on the bottom plate is the best location. The sensitivity of the results to the volume of the droplet was found to be very insignificant. For the setup used in this study, the optimal configuration for HS and the DMF device found to be a surface area as large as 13.3% of the area of the actuating electrodes for a superhydrophilic (Au_m and SiO_2) and over 22.2% for a hydrophilic surface (Au).

Finally, the best configuration found in the study for the hydrophilic spot (HS) was used for the fabrication of a capacitive biosensor for the detection of *Cryptosporidium*. Detection of different concentrations of *Cryptosporidium* was carried out with successful droplet removal from the surface of the sensor.

References

Alizadeh T. and Akbari A., 2013, Biosensors and Bioelectronics,43, 321–327.

Berggren C., Bjarnason B. and Johansson G., 2001, Electroanalysis, 13, 173-180.

Cho S. K., Moon H. J. and Kim C. J., 2013, J. Microelectromech. Syst., 12, 70–80.

Choi K., Kim J. Y., Ahn J. H., Choi J. M., Im M. and Choi Y. K., 2012, Lab. Chip., 12, 1533–1539.

Choi K., Ng A. H. C., Fobel R. and Wheeler A. R., 2012, Annu. Rev. Anal. Chem., 5, 413-440.

Fair R. B., Khlystov A., Tailor T. D., Ivanov V., Evans R. D., Griffin P. B., Srinivasan V., Pamula V. K., Pollack M. G. and Zhou J., 2007, Design & Test of Computers, IEEE, 24, 10-24.

Fan S. K., Hsieha T. H. and Lin D. Y.,2009, Lab Chip, 9, 1236-1242.

Fair R. B., 2007, Microfluid Nanofluid, 3, 245-281.

Franke T., Abate A. R., Weitz D. A. and Wixforth A., 2009, Lab. Chip., 9, 2625–7.

Labib M., Hedström M., Amin M. and Mattiasson B., 2009, Anal Bioanal Chem, 393, 1539–1544.

Luk V. N., Mo G. C. and Wheeler A. R., 2008, Langmuir, 24, 6382-6389.

Luka G., Ahmadi A., Najjaran H., Alocilja E., DeRosa M., Wolthers K., Malki A., Aziz H., Althani A., Hoorfar M., 2015, Sensors, 15, 30011-30031.

Malic L., Brassard D., Veres T. and Tabrizian M., 2010, Lab. Chip., 10, 418-431.

Malic L., Veres T. and Tabrizian M., 2011, Biosensors and Bioelectronics, 26 2053-2059.

Mugele F. and Baret J. C., 2005, J. Phys.: Condens. Matter, 17, 705–774.

Rackus D. G., Shamsi M. H. and Wheeler A. R., 2015, Chem. Soc. Rev., 44, 5320-5340.

Rezaei Nejad H., Samiei E., Ahmadi A. and Hoorfar M., 2015, RSC Adv., 5, 35966–35975.

Samiei E. and Hoorfar M., 2015, J. Micromech. Microeng., 25, 055008.

Samiei E., Rezaei Nejad H., and Hoorfar M., 2015, Appl. Phys. Lett., 106, 204101.

Srinivasan V., Pamula V.K., and Fair R. B., 2004, Lab. Chip., 4, 310-315.

Tavana H., Jehnichen D., Grundke K., Hair M. L. and Neumann A. W., 2007, Advances in Colloid and Interface Science, 134–135, 236–248.

Yi U. C. and Kim C. J., 2006, J. Micromech. Microeng. 16, 2053.

Yu Y., Chen J. and Zhou J., 2014, J. Micromech. Microeng., 24, 015020, 2014.

Highlights:

1- Surface properties of biosensors on digital microfluidics has been characterized.
2- Feasibility of droplet transport over the biosensor was investigated.
3- An optimized geometry was found for the biosensor with the largest possible area.
4- Capacitive detection of *Cryptosporidium* was performed as a proof of concept.